

initiated by quenching the protein from a high temperature to a low temperature. The dynamics of folding is found to occur in stages, reflecting the rugged energy landscape that the folding faces. This ruggedness is to be contrasted with the nearly smooth landscape that we found for models with simpler potentials. The FRET efficiency at low temperature shows a broad distribution signifying many trapped and misfolded states which may originate from the underlying rugged energy landscape. The multistage dynamics is reflected in the decay of survival probability. In particular, FRET is sensitive to the late stage of changes in the radius of gyration. This late stage dynamics is driven mainly by the change in topological pair-contact formation.

1. Förster, Th., Zwischenmolekulare energiewanderung und fluoreszenz. *Ann. Phys. (Leipzig)*, 1948, **2**, 55–75.
2. Telford, J. R., Wittung-Stafshede, P., Gray, H. B. and Winkler, J. R., Protein folding triggered by electron transfer. *Acc. Chem. Res.*, 1998, **31**, 755–763; Pascher, T., Chesick, J. P., Winkler, J. R. and Gray, H. B., Protein folding triggered by electron transfer. *Science*, 1996, **271**, 1558–1560.
3. Lyubovitsky, J. G., Gray, H. B. and Winkler, J. R., Mapping the cytochrome C folding landscape. *J. Am. Chem. Soc.*, 2002, **124**, 5481–5485.
4. Lakshmikanth, G. S., Sridevi, K., Krishnamoorthy, G. and Udgaonkar, J. B., Structure is lost incrementally during the unfolding of barstar. *Nat. Str. Biol.*, 2001, **8**, 799–804.
5. Srinivas, G. and Bagchi, B., Detection of collapsed and ordered polymer structures by fluorescence resonance energy transfer in stiff homopolymers: Bimodality in the reaction efficiency distribution. *J. Chem. Phys.*, 2002, **116**, 837–844.
6. Srinivas, G., Yethiraj, A. and Bagchi, B., FRET by FET and dynamics of polymer folding. *J. Phys. Chem.*, 2001, **B105**, 2475–2478.
7. Duan, Y. and Kollman, P. A., Pathways to a protein folding intermediate observed in a 1-microsecond simulation in aqueous solution. *Science*, 1998, **282**, 740–744.
8. Fernandez, A., Shen, M., Colubri, A., Sosnick, T. R., Berry, R. S. and Freed, K. F., Large-scale context in protein folding: villin headpiece. *Biochemistry*, 2003, **42**, 664–671.
9. Mukherjee, A. and Bagchi, B., Correlation between rate of folding, energy landscape, and topology in the folding of a model protein HP-36. *J. Chem. Phys.*, 2003, **118**, 4733.
10. Mukherjee, A. and Bagchi, B., Multistage contact pair dynamics during folding of model proteins. *J. Chem. Phys.* (submitted).
11. Liwo, A., Oldziej, S., Pincus, M. R., Wawak, R. J., Rackovsky, S. and Scheraga, H. A., A united-residue force field for off-lattice protein-structure simulations. I. Functional forms and parameters of long-range side-chain interaction potentials from protein crystal data. *J. Comput. Chem.*, 1997, **18**, 8849–8873.
12. Scheraga, H. A. *et al.*, Recent improvements in prediction of protein structure by global optimization of a potential energy function. *Proc. Natl. Acad. Sci. USA*, 2001, **98**, 2329–2333; Lee, J., Liwo, A. and Scheraga, H. A., Conformational space annealing and an off-lattice united-residue force field: application to the 10–55 fragment of staphylococcal protein A and to apo calbindin D9K. *Proc. Natl. Acad. Sci. USA*, 1999, **96**, 2025–2030.
13. Levitt, M. and Warshel, A., Computer simulation of protein folding. *Nature*, 1975, **253**, 694–698; Levitt, M., A simplified representation of protein conformations for rapid simulation of protein folding. *J. Mol. Biol.*, 1976, **104**, 59–107.
14. Kyte, J. and Doolittle, R. F., A simple method for displaying the hydrophobic character of a protein. *J. Mol. Biol.*, 1982, **157**, 105–132.
15. Zimm, B. H. and Bragg, J. K., Theory of the phase transition between helix and random coil in polypeptide chains. *J. Chem. Phys.*, 1959, **31**, 526–535.
16. Pace, C. N. and Scholtz, J. M., A helix propensity scale based on experimental studies of peptides and proteins. *Biophys. J.*, 1998, **75**, 422.
17. Chou, P. Y. and Fasman, G., Conformational parameters for amino acids in helical, beta-sheet, and random coil regions calculated from proteins. *Biochemistry*, 1974, **13**, 211–222.
18. Mooij, G. C. A. M., Frenkel, D. and Smit, B., Direct simulation of phase equilibria of chain molecules. *J. Phys. Condens. Matter*, 1992, **4**, L255–L259; Frenkel, D. and Smit, B., Unexpected length dependence of the solubility of chain molecules. *Mol. Phys.*, 1992, **75**, 983–988.
19. Ermak, D. L. and McCammon, J. A., Brownian dynamics with hydrodynamic interactions. *J. Chem. Phys.*, 1978, **69**, 1352–1360.
20. Hansen, J. P. and McDonald, I. R., *Theory of Simple Liquids*, Academic Press, 1986.
21. Deniz, A. A. *et al.*, Single molecule protein folding: diffusion Forster energy transfer studies of the denaturation of Chymotrypsin inhibitor 2. *Proc. Natl. Acad. Sci. USA*, 2000, **97**, 5179–5184.
22. Deniz, A. A. *et al.*, Radiometric single pair FRET on freely diffusing molecules – observation of Forster distance dependence and of sub-populations. *Proc. Natl. Acad. Sci. USA*, 1999, **96**, 3670–3675.
23. Srinivas, G. and Bagchi, B., Energy transfer efficiency distributions in polymers in solution during folding and unfolding. *Phys. Chem. Commun.*, 2002, **5**, 59–62.

ACKNOWLEDGEMENTS. We thank CSIR, DAE and DST, New Delhi for financial support. A.M. thanks Ashwin, Kausik, Prasanth, Rajesh, Dwaipayan and Swapan for help and discussions.

Received 28 March 2003; revised accepted 21 May 2003

## Electrodynamic confinement of europium ions

Pushpa M. Rao\*, Soumen Bhattacharya, S. G. Nakhate and Gopal Joshi<sup>†</sup>

Spectroscopy Division, <sup>†</sup>Electronics Division, Bhabha Atomic Research Centre, Mumbai 400 085, India

**Europium ions were trapped in a Paul trap. The trapped ions were detected electronically, which involved the damping of a weakly excited tank circuit across the trap electrodes, tuned to one of the ion frequencies in the trap. The storage time of the trapped ions was observed to be 8 s at  $2.4 \times 10^{-6}$  Pa base vacuum. On cooling the ions with nitrogen as buffer gas at  $1.8 \times 10^{-4}$  Pa and helium at  $6.4 \times 10^{-5}$  Pa, the storage time improved to 41.4 s and 102.7 s respectively.**

THE confinement of an ensemble of free ions allowing the observation of isolated charge particles, even that of a single ion requires novel techniques as reported in *The technique of ion trapping*. During the last two decades, there has been a tremendous progress in the techniques of trapping and cooling of ions in the quadrupole ion traps. A single ion has been trapped and observed over a long period of time enabling the measurement of its properties with an extremely high accuracy in the fields of atomic physics, quantum optics and nuclear physics<sup>1–4</sup>.

\*For correspondence. (e-mail: pushpam@magnum.barc.ernet.in)

We have initiated the setting-up of ion traps with a view to carrying out precision spectroscopic studies of trapped ions. The quadrupole ion trap was used in the Penning mode as an initial test case and electrons were trapped successfully<sup>5</sup>. In this short note, we describe the trapping and non-destructive electronic detection of europium ions.

We have used a quadrupole trap, which essentially consists of three electrodes whose surfaces are hyperboloids of revolution about the  $z$ -axis<sup>5</sup>. The ions are confined electrostatically wherein an oscillating potential  $V_{ac} \cos(\Omega t)$  in conjunction with a static potential  $U_{dc}$ , is applied to the ring electrode. Applying a potential  $\phi_0$  between the end caps and the ring electrode, gives rise to a quadrupole electric potential of cylindrical symmetry of the form

$$\phi(r, z) = \frac{\phi_0}{2r_0^2} [x^2 + y^2 - 2z^2], \quad (1)$$

where  $r_0$  is the ring electrode radius. The trap is operated in the Paul mode when the potential  $\phi_0$  is of the form  $U_{dc} + V_{ac} \cos(\Omega t)$ . The equations of motion of the ions then are described by a set of Mathieu equations

$$\frac{d^2 x_i}{d\tau^2} + (a_i - 2q_i \cos 2\tau) x_i = 0; \quad i = r, z \quad (2)$$

$$-a_z = 2a_r = \frac{8eU_{dc}}{m\Omega^2 r_0^2}; \quad q_z = -2q_r = \frac{4eV_{ac}}{m\Omega^2 r_0^2};$$

$$\tau = \frac{1}{2}\Omega t,$$

where  $m$  and  $e$  are the mass and electric charge of the ion,  $V_{ac}$  and  $\Omega/2\pi$  the amplitude and frequency of the oscillating potential.

The Mathieu equations have two types of solutions, which lead to both stable and unstable ion motions. In the stable motion, the ion oscillates both in the  $r$  and  $z$  directions with limited amplitudes, without hitting the electrodes. In the unstable motion, the amplitudes of oscillation grow exponentially either in any one of the directions, or in both and thus the ions are not confined. The stability of the ion motions, depends purely on  $a$  and  $q$  parameters<sup>6</sup>. Figure 1 shows the  $a$  and  $q$  map and the shaded area is the first stability region. Choosing  $a$  and  $q$  parameters and hence the operating parameters from within this region ensures the stability of the ion motion and results in the confinement of ions.

In general, the solutions to the equations of motion (2) are complicated. However when  $a \ll q \ll 1$ , an approximate solution can be found<sup>7</sup>. It is seen mathematically, that the motion of the ions can be described as slow (secular) oscillation with the fundamental frequencies  $\omega_{r,z} = \beta_{r,z}\Omega/2$ , which is modulated with a micromotion – a much faster oscillation – of the driving frequency  $\Omega$ , neglecting the higher harmonics. Here,  $\beta_{r,z}$  is a function

of only the Mathieu parameters  $a$  and  $q$ , i.e.  $\beta_{r,z} = a_{r,z} + q_{r,z}^2$ .

The ring electrode radius of the quadrupole trap used is 20 mm and the end caps separation is 14.1 mm. The lower end cap has two slits to accommodate the platinum filament and the upper end cap is in the form of a mesh. The trap is placed in a UHV chamber operated at  $2.4 \times 10^{-6}$  Pa base pressure using a turbomolecular and an ion pump. Provision is made for the introduction of buffer gas into the chamber through a needle valve. A few milligrams of europium metal is placed on the platinum filament and resistive heating of the filament results in the production of  $\text{Eu}^+$  ions by the process of surface ionization.

Ions are created and maintained in stable trajectories with an oscillating potential of amplitude 820  $V_{pp}$ , frequency 472.6 KHz and static potential about 5 V. The trapped ions are detected electronically (Figure 2 a) using

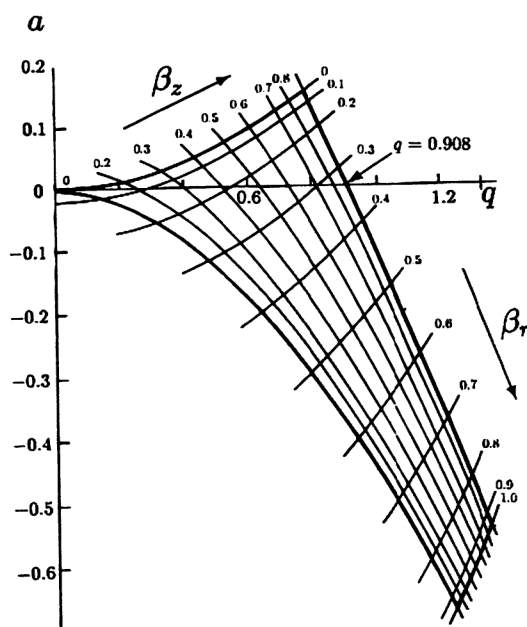


Figure 1. Stability diagram in the  $a$ - $q$  plane of the Mathieu equation for simultaneous confinement of ions in the  $r$  and  $z$  directions.

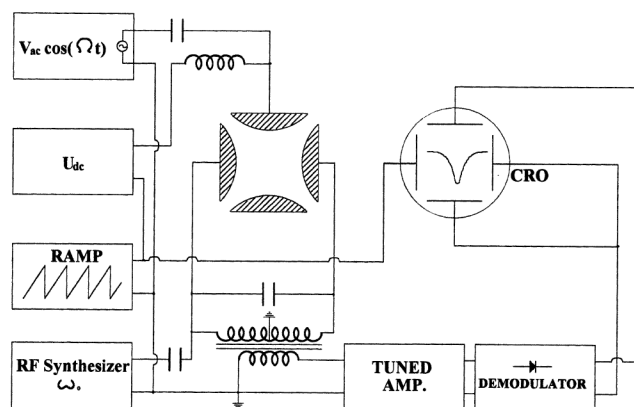
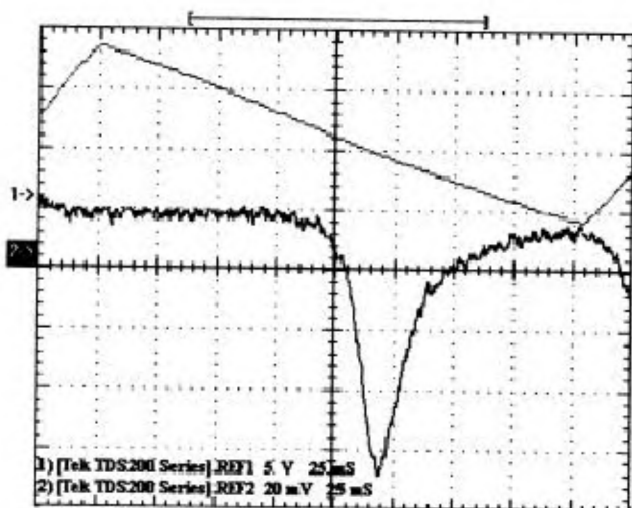
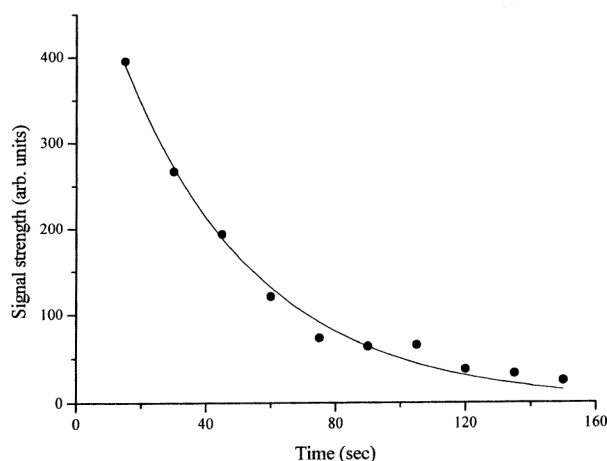


Figure 2 a. Schematic diagram of the experimental set-up.



**Figure 2 b.** Oscilloscope trace of the applied ramp voltage at the ring electrode and the rf absorption signal of the trapped  $\text{Eu}^+$  ions.



**Figure 2 c.** Decay of the trapped  $\text{Eu}^+$  ion population (cooled with nitrogen at  $1.8 \times 10^{-4}$  Pa) with time. The filled circles are experimental points and the continuous curve is the least squares fit to the exponential function.

a high impedance (2.5 Mega-ohm) tank circuit connected across the end caps of the trap. The mid-point of the tank circuit is grounded to minimize the interference due to the high voltage source  $V_{ac}$ . The tank circuit is tuned and weakly coupled to a rf source fixed at frequency  $\omega_0$  close to the z-motion of ions' oscillation frequency  $\omega_z$  (secular frequency). The secular frequency  $\omega_z$  of the trapped ions depends on the trapping parameters ( $V_{ac}$ ,  $U_{dc}$  and  $\Omega$ ). Therefore, by ramping the dc voltage ( $U_{dc}$ ), the secular frequency of the ions is brought into resonance with the detection frequency  $\omega_0$  of the tank circuit. At resonance, the trapped ions absorb energy from the rf source resulting in a voltage drop across the tank circuit. This voltage is further amplified and demodulated by a high impedance-tuned amplifier followed by an amplitude

demodulator, which is magnetically coupled to the tank circuit. The typical rf absorption signal of the trapped  $\text{Eu}^+$  ions is shown in Figure 2 b.

As expected, the ion loss is observed to be exponential with time (Figure 2 c). The storage time constant is defined as the time interval in which the ion population decreases to  $e^{-1}$  of its initial value. The storage time of the trapped  $\text{Eu}^+$  ions is observed to be 8 s at  $2.4 \times 10^{-6}$  Pa base pressure. The temperature of the trapped ions is usually thousands of degrees kelvin due to rf heating from the applied trapping potential. Hot ions are more easily lost through collisions with the background gases than the cold ions, thus reducing their storage time. Cooling the ions improves the storage time. Collisional cooling is one of the simplest methods wherein the hot ions are cooled with a gas of lower temperature by exchange of energy. The amount of energy transfer depends on the mass of the buffer gas relative to the trapped ions, its temperature and pressure. When the ratio of mass of trapped ion ( $m_i$ ) to that of the buffer gas ( $m_b$ ) is much greater than 1; i.e.  $m_i/m_b \gg 1$ , collisions will essentially result in a viscous drag which lowers the mean kinetic energy of ions<sup>8</sup>. In the Paul trap, the energy transfer is limited by the ion-ion collisions, perturbations in the applied potential and the amplitude of the external rf-excitation used in the process of electronic detection.

The trapped  $\text{Eu}^+$  ions were cooled using buffer gases of different masses. Cooling the ions with nitrogen at optimized pressure of  $1.8 \times 10^{-4}$  Pa, the storage time is found to be  $41.4 \pm 2.0$  s. The storage time is further improved to  $102.7 \pm 3.6$  s, using helium as buffer gas at the optimized pressure of  $6.4 \times 10^{-5}$  Pa.

1. Piek, E., Hollemann, G. and Walther, H., Laser cooling and quantum jumps of a single indium ion. *Phys. Rev.*, 1994, **A49**, 402–408.
2. Itano, W. M., Heinze, D. J., Bollinger, J. J. and Wineland, D. J., Quantum Xeno effect. *Phys. Rev.*, 1990, **A41**, 2295–2300.
3. Bollen, G., High accuracy mass spectrometry, nuclear shapes and nuclear structures at low excitation energies. Proceedings of NATO Advance Research Workshop, 1993, p. 399.
4. Enders, K. *et al.*, Hyperfine structure measurements in the ground state of radioactive  $^{150}\text{Eu}^+$  ions. *Phys. Rev.*, 1995, **A52**, 4434–4438.
5. Rao Pushpa, M., D'Souza, R., Joshi Gopal and Ahmad, S. A., Confinement of electrons in a Penning trap. *Curr. Sci.*, 1999, **76**, 34–35.
6. Rao Pushpa, M., D'Souza, R. and Ahmad, S. A., Quadrupole ion traps. *Resonance*, 2001, **6**, 22–37.
7. Wukker, R. F., Shelton H. and Langamur, R. V., Electrodynamic containment of charged particles by three-phase voltages. *J. Appl. Phys.*, 1959, **30**, 342–349.
8. Major, F. G. and Dehmelt, H. G., Exchange-collision technique for rf spectroscopy of stored ions. *Phys. Rev.*, 1968, **170**, 91–107.

**ACKNOWLEDGEMENTS.** We thank Dr N. C. Das for his unstinted support and constant encouragement during the course of this work. We also thank Dr S. K. Kataria for his immense cooperation and help.

Received 20 January 2003; revised accepted 10 March 2003